mathematics

MDPI

Article

A New X-Bar Control Chart for Using Neutrosophic Exponentially Weighted Moving Average

Muhammad Aslam [1,*], Ali Hussein AL-Marshadi [1] and Nasrullah Khan [2]

[1] Department of Statistics, Faculty of Science, King Abdulaziz University, Jeddah 21551, Saudi Arabia; aalmarshadi@kau.edu.sa
[2] Department of Statistics, University of Veterinary and Animal Sciences, Jhang Campus, Lahore 54000, Pakistan; nas_shan1@hotmail.com
* Correspondence: aslam_ravian@hotmail.com

Received: 22 August 2019; Accepted: 8 October 2019; Published: 12 October 2019

Abstract: The existing Shewhart X-bar control charts using the exponentially weighted moving average statistic are designed under the assumption that all observations are precise, determined, and known. In practice, it may be possible that the sample or the population observations are imprecise or fuzzy. In this paper, we present the designing of the X-bar control chart under the symmetry property of normal distribution using the neutrosophic exponentially weighted moving average statistics. We will first introduce the neutrosophic exponentially weighted moving average statistic, and then use it to design the X-bar control chart for monitoring the data under an uncertainty environment. We will determine the neutrosophic average run length using the neutrosophic Monte Carlo simulation. The efficiency of the proposed plan will be compared with existing control charts.

Keywords: neutrosophic logic; fuzzy logic; control chart; neutrosophic numbers; monitoring

1. Introduction

The production process may shift from the target due to a number of reasons. Therefore, to produce the product according to given specifications, it is watched to indicate any shift in the process. The control charts are popularly used in the industry to watch the production process. In the industries, usually, the Shewhart control charts are used for the monitoring of the process. Although these control charts have a simple operational procedure, they are unable to detect a small shift in the process. Therefore, the Shewhart control charts do not detect a very small shift, and cause a high non-conforming product. The applications of such charts can be seen in [1–6].

The control charts using the exponentially weighted moving average (EWMA) used the current subgroup and previous subgroup information, and were said to be more efficient in detecting a very small shift in the process. The control chart based on this statistic is more efficient than the traditional Shewhart control charts. Roberts [7] designed a control chart using this statistic first time. Haq [8] and Haq et al. [9,10] used the EWMA statistic to propose a variety of control charts. Abbasi et al. [11] and Abbasi [12] introduced its setting in normal and non-normal situations and for measurement errors, respectively. Sanusi et al. [13] presented an alternative for the EWMA-based chart when additional information about the main variable is available. References [14–17] presented such control charts. More basic information about the control charts can be seen in [18,19].

The traditional Shewhart control charts cannot be applied when uncertainty or randomness is expected in the data. The fuzzy-based control charts are the best alternative to monitor the process when observations or the parameters under study are fuzzy. As mentioned by Khademi and Amirzadeh [20], "Fuzzy data exist ubiquitously in the modern manufacturing process"; therefore, serval authors paid attention to work on such control charts, such as for example [21–26].

The traditional fuzzy logic is a special case of neutrosophic logic. The latter one has the ability to deal with the measure of indeterminacy; see Smarandache [27]. The classic statistics (CS) method is applied under the assumption that all observations in data are determined, precise, and certain. However, in the modern manufacturing process, it may not be possible to record all determined observations in the data. In this situation, the neutrosophic statistics (NS) can be applied for the analysis of the data. The NS was introduced by Smarandache [28] using neutrosophic logic, which is the generation of CS. The NS is more effective to be applied for the analysis of imprecise data than CS. Chen et al. [29,30] proved the effectiveness of the NS-based analysis. Aslam [31] introduced a new area of neutrosophic quality control (NQC). Aslam et al. [32,33] introduced NS-based attributes and variable charts. Aslam and Khan [34] proposed the X-bar chart under NS. Aslam et al. [35] designed a chart to monitor reliability under uncertainty. Aslam [36,37] proposed the attribute and variable charts using resampling under NS.

Şentürk et al. [38] proposed the EWMA control chart using the fuzzy approach, which is the special case of the control chart using the neutrosophic logic, as mentioned by Smarandache [27]. By looking into the literature of the control chart under the uncertainty environment, we did not find any work on the X-bar control chart based on the neutrosophic exponentially weighted moving average (NEWMA). In this paper, we will first introduce NEWMA. We will introduce the new Monto Carlo simulation under the neutrosophic statistical interval method (NSIM). We will determine the neutrosophic average run length (NARL) of the proposed chart to compare its performance. We hope that the proposed chart will be more sensitive in detecting a small shift in the process as compared to the traditional Shewhart X-bar chart, EWMA X-bar chart under CS [19] and X-bar chart under NS [34].

2. The Proposed NEWMA Statistics

In this section, we will introduce NEWMA statistics. Let $\overline{X}_N \epsilon \left[\frac{\sum_{i=1}^{n_L} X_i}{n_L}, \frac{\sum_{i=1}^{n_U} X_i}{n_U} \right]$; $\overline{X}_N \epsilon \left\{ \overline{X}_L, \overline{X}_U \right\}$ be the neutrosophic sample average of a neutrosophic random variable (nrv) $X_{iN} \epsilon \{X_L, X_U\} = i =$ 1,2,3, … , n_N, where n_N is the neutrosophic sample size. Suppose that $S_N^2 = \sum_{i=1}^{n_N} \left(X_N - \overline{X}_N \right)^2 / n_N - 1$; $S_N^2 \epsilon \left\{ S_L^2, S_L^2 \right\}$ represents the neutrosophic sample variance. By following Smarandache [28] and Aslam [31], the neutrosophic sample average follows the neutrosophic normal distribution (NND) with a neutrosophic population mean $\mu_N = \sum_{i=1}^{N_N} X_N / N_N$; $\mu_N \epsilon \{\mu_L, \mu_U\}$ and neutrosophic population variance $\sigma_N^2 = \left[\left\{ \sum_{i=1}^{n_N} (X_N - \mu_N)^2 / N_N - 1 \right\} / n_N \right]$; $\sigma_N^2 \epsilon \left\{ \sigma_L^2 / n_N, \sigma_L^2 / n_N \right\}$. Based on the given information, we define NEWMA statistics as follows:

$$EWMA_{N,i} = \lambda_N \overline{X}_N + (1 - \lambda_N) EWMA_{N,i-1};\ EWMA_{N,i} \epsilon \left\{ EWMA_{L,i}, EWMA_{U,i} \right\} \quad (1)$$

where $\lambda_N \epsilon \{\lambda_L, \lambda_U\}$; $[0,0] \leq \lambda_N \leq [1,1]$ denotes the neutrosophic smoothing constant. Note here that $\overline{X}_N \epsilon \left\{ \overline{X}_L, \overline{X}_U \right\}$ are assumed to be independent random variables with neutrosophic variance σ_N^2 / n_N ($\sigma_N^2 \epsilon \left\{ \sigma_L^2 / n_N, \sigma_L^2 / n_N \right\}$ and known neutrosophic population variance, as shown in [38]. The setting of $\lambda_N \epsilon \{\lambda_L, \lambda_U\}$ is matter of personal experience. Montgomery [14] recommended that it should be selected from 0.05 to 0.25. The $EWMA_{N,i}$ follows the NND with neutrosophic mean $\mu_N \epsilon \{\mu_L, \mu_U\}$ and neutrosophic standard deviation $\frac{\sigma_N}{\sqrt{n_N}} \sqrt{\frac{\lambda_N}{2 - \lambda_N}}$.

3. The Proposed NEWMA X-Bar Control Chart

The proposed X-bar control chart using the NS is described as follows:

1. Choose a random sample of size $n_N \epsilon \{n_L, n_U\}$ and compute $EWMA_{N,i}$ statistics.

$$EWMA_{N,i} = \lambda_N \overline{X}_N + (1 - \lambda_N) EWMA_{N,i-1};\ EWMA_{N,i} \epsilon \left\{ EWMA_{L,i}, EWMA_{U,i} \right\}$$

2. Declare the process is an in-control state if $LCL_N < EWMA_{N,i} < UCL_N$; otherwise, it is in an out-of-control state. Note here that $LCL_N \epsilon [LCL_L, LCL_U]$ and $LCU_N \epsilon [LCU_L, LCU_U]$ are the neutrosophic lower and upper control limits.

The proposed chart becomes a chart based on NS proposed by Aslam and Khan [34] when $\lambda_N \epsilon \{1, 1\}$. When all the observations are precise, the proposed chart becomes the traditional Shewhart chart under CS. The neutrosophic control limits are given by:

$$LCL_N = \mu_N - k_N \frac{\sigma_N}{\sqrt{n_N}} \sqrt{\frac{\lambda_N}{2 - \lambda_N}};\ LCL_N \epsilon [LCL_L, LCL_U],\ k_N \in \left\{k_{L,}, k_U\right\},\ \mu_N \in \left\{\mu_{L,}, \mu_{U,}\right\} \tag{2}$$

$$UCL_N = \mu_N + k_N \frac{\sigma_N}{\sqrt{n_N}} \sqrt{\frac{\lambda_N}{2 - \lambda_N}};\ LCU_N \epsilon [LCU_L, LCU_U],\ k_N \in \left\{k_{L,}, k_U\right\},\ \mu_N \in \left\{\mu_{L,}, \mu_{U,}\right\} \tag{3}$$

where $k_N \in \left\{k_{L,}, k_U\right\}$ is the neutrosophic control limits coefficient, and will be determined later. Let $\mu_{0N} \epsilon \{\mu_{0L}, \mu_{0U}\}$ be the target value for the process. According to the operational process of the proposed control, the probability that the process under the NS is an in-control state is given by:

$$P^0_{inN} = P\left(LCL_N \le \overline{X} \le UCL_N / \mu_{0N}\right);\ \mu_{0N} \epsilon \{\mu_{0L}, \mu_{0U}\} \tag{4}$$

The neutrosophic average run length (NARL) of the proposed chart is given by:

$$ARL_{0N} = \frac{1}{1 - P^0_{inN}};\ ARL_{0N} \epsilon \{ARL_{0L}, ARL_{0U}\} \tag{5}$$

Suppose now that the process has shifted to a new target at $\mu_{1N} = \mu_{0N} + d\sigma_N;\ \mu_{1N} \epsilon \{\mu_{1L}, \mu_{1U}\}$, where d is the shift constant. The neutrosophic probability of an in-control state at $\mu_{1N} \epsilon \{\mu_{1L}, \mu_{1U}\}$ is given by:

$$P^1_{in} = P\left(LCL_N \le \overline{X}_N \le UCL_N / \mu_{N1} = \mu_N + \mathrm{d}\sigma_N\right);\ \mu_{1N} \epsilon \{\mu_{1L}, \mu_{1U}\}.$$

The NARL at $\mu_{1N} \epsilon \{\mu_{1L}, \mu_{1U}\}$ is defined by:

$$ARL_{1N} = \frac{1}{1 - P^1_{in}};\ ARL_{1N} \epsilon \{ARL_{1L}, ARL_{1U}\} \tag{6}$$

4. The Proposed Neutrosophic Monte Carlo Simulation (NMCS)

As we mentioned earlier, the neutrosophic control limits coefficient $k_N \epsilon \left\{k_{L,}, k_U\right\}$ will be determined through the neutrosophic Monte Carlo Simulation (NMCS) under the given constraints. The proposed NMCS is stated as follows.

4.1. For In-Control State

Step 1: A random sample of size $n_N \epsilon \{n_L, n_U\}$ is generated from a standard normal distribution. The mean of the random sample interval of size $n_N \epsilon \{n_L, n_U\}$ is computed as $\overline{X}_N \epsilon \left\{\overline{X}_L, \overline{X}_U\right\}$ is computed. The plotting $EWMA_{N,i}$ statistic is computed as:

$$EWMA_{N,i} = \lambda_N \bar{x}_N + (1 - \lambda_N) EWMA_{N,i-1}$$

Step 2: The proposed statistic $EWMA_{N,i}$ is plotted over the $LCL_N \epsilon [LCL_L, LCL_U]$ and $LCU_N \epsilon [LCU_L, LCU_U]$ by selecting a suitable value of $k_N \epsilon \left\{k_{L,}, k_U\right\}$, and $ARL_{0N} \epsilon \{ARL_{0L}, ARL_{0U}\}$ is computed.

Step 3: The $ARL_{0N} \epsilon \{ARL_{0L}, ARL_{0U}\}$ and neutrosophic standard deviation (NSD) are computed by iterating process 10,000; only those $k_N \epsilon \left\{k_{L,}, k_U\right\}$ values along with their respective parameters

are selected for which $ARL_{0N} = r_{0N}$; $ARL_{0N}\epsilon\{ARL_{0L}, ARL_{0U}\}$, where r_{0N} is the specified value of $ARL_{0N}\epsilon\{ARL_{0L}, ARL_{0U}\}$.

4.2. For Shifted Process

Step 1: For selected values of $k_N\epsilon\left\{k_{L,}, k_U\right\}$ and their corresponding parameters, $LCL_N\epsilon[LCL_L, LCL_U]$ and $LCU_N\epsilon[LCU_L, LCU_U]$ constructed.

Step 2: As per explained for the in control process in step 1, now data is generated at $\mu_{1N}\epsilon\{\mu_{1L}, \mu_{1U}\}$ and plotted on $LCL_N\epsilon[LCL_L, LCL_U]$ and $LCU_N\epsilon[LCU_L, LCU_U]$, and $ARL_{1N}\epsilon\{ARL_{1L}, ARL_{1U}\}$ is computed.

Step 3: The $ARL_{1N}\epsilon\{ARL_{1L}, ARL_{1U}\}$ is computed for a specified shift level by 10,000 iterations of the process.

Step 4: For various shifts, levels step 2 and 3 are repeated, the values $ARL_{1N}\epsilon\{ARL_{1L}, ARL_{1U}\}$ and NSD are computed at various values of d.

Note here that the proposed NMCS is the generalization of Monte Carlo simulation under CS. The values of $ARL_{1N}\epsilon\{ARL_{1L}, ARL_{1U}\}$ and NSD are determined for various values of d, $n_N\epsilon\{n_L, n_U\}$ and $\lambda_N\epsilon\{\lambda_L, \lambda_U\}$ $ARL_{0N}\epsilon\{ARL_{0L}, ARL_{0U}\}$, and are shown in Tables 1–4 for $ARL_{0N}\epsilon\{300, 300\}$ rather than $ARL_{0N}\epsilon\{370, 370\}$. The values of NARL when $n_N\epsilon[3, 5]$ and $\lambda_N\epsilon[0.08, 0.12]$ are shown in Table 1. The values of NARL when $n_N\epsilon[3, 5]$ and $\lambda_N\epsilon[0.18, 0.22]$ are shown in Table 2. The values of NARL when $n_N\epsilon[3, 5]$ and $\lambda_N\epsilon[0.28, 0.32]$ are shown in Table 3. The values of NARL when $n_N\epsilon[5, 10]$, $n_N\epsilon[5, 8]$, and $\lambda_N\epsilon[0.08, 0.12]$ are given in Table 4. From Tables 1–4, it is worth to note that when all other parameters are constant, the values of NSD are smaller for $ARL_{0N}\epsilon\{300, 300\}$ than for $ARL_{0N}\epsilon\{370, 370\}$. With the increase in $\lambda_N\epsilon\{\lambda_L, \lambda_U\}$, we note the decreasing trend in $ARL_{1N}\epsilon\{ARL_{1L}, ARL_{1U}\}$ and increasing trend in NSD. From Table 4, we observe that the indeterminacy interval in $ARL_{1N}\epsilon\{ARL_{1L}, ARL_{1U}\}$ increases as $n_N\epsilon\{n_L, n_U\}$ increases from $n_N\epsilon$ [5,8] to $n_N\epsilon$ [5,10]. On the other hand, the indeterminacy interval in NSD deceases as $n_N\epsilon\{n_L, n_U\}$ increases.

Table 1. The values neutrosophic average run length (NARL) and neutrosophic standard deviation (NSD) when $n_N\epsilon[3, 5]$ and $\lambda_N\epsilon[0.08, 0.12]$.

k_N	[2.565,2.675]		[2.655,2.765]	
d	**NARL**	**NSD**	**NARL**	**NSD**
0	[306.19,301.49]	[288.72,289.56]	[368.28,376.77]	[345.26,354.91]
0.05	[220.34,202.5]	[206.84,195.15]	[270.32,248.92]	[257.15,238.27]
0.1	[121.84,99.72]	[109.75,93.06]	[141.33,117.16]	[130.78,106.3]
0.15	[71.34,53.39]	[61.32,45.2]	[80.28,61.22]	[68.96,53.3]
0.2	[45.6,33.38]	[36.07,25.93]	[50.59,36.58]	[39.41,28.44]
0.25	[32.02,22.68]	[22.98,15.89]	[34.7,24.71]	[24.42,17.5]
0.3	[24.18,16.77]	[15.29,10.67]	[25.78,18.28]	[16.59,11.86]
0.4	[15.69,10.75]	[8.58,5.6]	[16.62,11.53]	[9.06,6.2]
0.5	[11.67,8]	[5.47,3.69]	[12.24,8.19]	[5.83,3.66]
0.6	[9.16,6.21]	[3.86,2.47]	[9.57,6.52]	[4,2.59]
0.7	[7.56,5.17]	[2.9,1.89]	[7.91,5.35]	[3.01,1.91]
0.8	[6.42,4.39]	[2.27,1.44]	[6.74,4.59]	[2.34,1.51]
0.9	[5.67,3.85]	[1.84,1.17]	[5.87,4]	[1.88,1.21]
1	[5.03,3.43]	[1.53,0.98]	[5.17,3.58]	[1.55,1.02]
1.25	[3.96,2.75]	[1.07,0.71]	[4.08,2.85]	[1.09,0.72]
1.5	[3.29,2.31]	[0.79,0.52]	[3.4,2.37]	[0.8,0.55]
1.75	[2.83,2.05]	[0.65,0.38]	[2.93,2.1]	[0.65,0.39]
2	[2.5,1.89]	[0.56,0.37]	[2.58,1.94]	[0.57,0.32]
2.5	[2.09,1.52]	[0.33,0.5]	[2.12,1.59]	[0.34,0.49]
3	[1.92,1.14]	[0.3,0.35]	[1.96,1.19]	[0.25,0.39]

Table 2. The values NARL and NSD when $n_N \epsilon [3,5]$ and $\lambda_N \epsilon [0.18, 0.22]$.

k_N	**[2.77,2.815]**		**[2.85,2.888]**	
d	**NARL**	**NSD**	**NARL**	**NSD**
0	[306.29,304.18]	[295.94,294.05]	[368.53,367.73]	[347.63,347.95]
0.05	[248.13,232.68]	[238.69,228.36]	[303.11,279.09]	[289.54,265.81]
0.1	[155.07,128.27]	[149.33,122.61]	[187.46,150.35]	[180.34,144.18]
0.15	[93.67,71.64]	[87.13,66.2]	[110.77,82.51]	[105.67,77.1]
0.2	[60.15,42.93]	[53.64,38.28]	[69.85,47.94]	[62.94,42.65]
0.25	[40.47,27.91]	[34.74,23.37]	[45.33,31.22]	[39.11,27.02]
0.3	[29.38,19.78]	[23.75,15.61]	[32.21,21.34]	[27.03,16.82]
0.4	[17.27,11.6]	[12.42,7.85]	[18.72,12.15]	[13.34,8.17]
0.5	[11.66,7.91]	[7.53,4.58]	[12.46,8.32]	[7.82,4.77]
0.6	[8.69,5.89]	[4.75,2.88]	[9.15,6.18]	[5.16,3.08]
0.7	[6.85,4.75]	[3.42,2.09]	[7.25,4.91]	[3.63,2.17]
0.8	[5.68,3.98]	[2.55,1.6]	[5.9,4.1]	[2.66,1.64]
0.9	[4.85,3.41]	[1.99,1.26]	[5.04,3.51]	[2.04,1.28]
1	[4.24,3.01]	[1.61,1.02]	[4.38,3.11]	[1.68,1.05]
1.25	[3.25,2.38]	[1.06,0.69]	[3.36,2.43]	[1.1,0.69]
1.5	[2.67,2]	[0.77,0.52]	[2.76,2.04]	[0.79,0.52]
1.75	[2.3,1.74]	[0.59,0.49]	[2.36,1.78]	[0.6,0.49]
2	[2.04,1.51]	[0.47,0.51]	[2.08,1.56]	[0.48,0.5]
2.5	[1.7,1.13]	[0.48,0.34]	[1.76,1.17]	[0.46,0.37]
3	[1.35,1.01]	[0.48,0.12]	[1.41,1.02]	[0.49,0.14]

Table 3. The values NARL and NSD when $n_N \epsilon [3,5]$ and $\lambda_N \epsilon [0.28, 0.32]$.

k_N	**[2.85,2.865]**		**[2.93,2.945]**	
d	**NARL**	**NSD**	**NARL**	**NSD**
0	[304.15,300.13]	[293.48,289.27]	[376.11,372.72]	[357.13,349.32]
0.05	[262.23,240.42]	[255.83,239.44]	[324.21,297.07]	[310.4,288.11]
0.1	[181.48,148.62]	[182.19,145.09]	[219.18,184.26]	[216.15,178.17]
0.15	[118.58,88.25]	[116.39,85.83]	[143.28,103.88]	[141.14,100.56]
0.2	[77.25,52.48]	[72.69,49.36]	[90.85,61.51]	[86.42,56.98]
0.25	[52.6,35.06]	[49.24,31.52]	[60.08,39.45]	[56.86,35.65]
0.3	[36.38,23.97]	[32.41,20.83]	[41.96,26.95]	[37.69,23.26]
0.4	[20.61,12.97]	[17.05,10.06]	[23.16,14.29]	[19.08,11.15]
0.5	[13.37,8.5]	[10.02,5.75]	[14.41,9.22]	[10.91,6.35]
0.6	[9.35,6.11]	[6.27,3.65]	[10.05,6.31]	[6.73,3.73]
0.7	[7.06,4.68]	[4.19,2.44]	[7.47,4.94]	[4.44,2.59]
0.8	[5.63,3.8]	[3.02,1.78]	[5.98,4]	[3.25,1.88]
0.9	[4.73,3.22]	[2.32,1.39]	[4.92,3.37]	[2.44,1.44]
1	[4.05,2.82]	[1.81,1.1]	[4.17,2.94]	[1.91,1.15]
1.25	[3.01,2.18]	[1.15,0.72]	[3.1,2.23]	[1.19,0.73]
1.5	[2.43,1.79]	[0.8,0.57]	[2.47,1.84]	[0.81,0.58]
1.75	[2.06,1.51]	[0.62,0.53]	[2.11,1.56]	[0.61,0.53]
2	[1.8,1.28]	[0.54,0.45]	[1.85,1.33]	[0.54,0.47]
2.5	[1.41,1.05]	[0.5,0.21]	[1.46,1.05]	[0.51,0.22]
3	[1.13,1]	[0.34,0.05]	[1.17,1]	[0.38,0.06]

Table 4. The values NARL and NSD when $n_N \epsilon [5, 10]$, $n_N \epsilon [5, 8]$,and $\lambda_N \epsilon [0.08, 0.12]$.

k_N	[5,8]	[2.658,2.765]	[5,10]	[2.66,2.77]
d	NARL	NSD	NARL	NSD
0	[377.43,374.68]	[353.08,351.51]	[378.24,375.35]	[351.52,352.17]
0.05	[225.26,200.98]	[211.29,190.39]	[222.54,184.41]	[214.36,176.53]
0.1	[100.64,81.77]	[88.74,75.56]	[100.83,66.16]	[88.44,57.36]
0.15	[52.67,40.17]	[42.89,32.77]	[53.58,33.15]	[42.82,25.6]
0.2	[32.94,24.23]	[23.17,17.19]	[33.03,19.79]	[23.32,12.94]
0.25	[23.34,16.54]	[14.33,10.43]	[23.03,13.78]	[14.25,8.06]
0.3	[17.43,12.48]	[9.54,7.04]	[17.43,10.48]	[9.7,5.39]
0.4	[11.62,8.17]	[5.38,3.74]	[11.7,7.06]	[5.43,2.93]
0.5	[8.69,6.08]	[3.43,2.32]	[8.75,5.3]	[3.49,1.9]
0.6	[6.98,4.86]	[2.49,1.64]	[6.97,4.25]	[2.46,1.33]
0.7	[5.83,4.07]	[1.83,1.24]	[5.84,3.61]	[1.9,1.03]
0.8	[5.05,3.52]	[1.49,0.99]	[5.03,3.14]	[1.47,0.84]
0.9	[4.39,3.11]	[1.2,0.83]	[4.41,2.79]	[1.21,0.71]
1	[3.95,2.79]	[1.01,0.7]	[3.96,2.51]	[1.01,0.6]
1.25	[3.17,2.26]	[0.74,0.49]	[3.17,2.09]	[0.73,0.38]
1.5	[2.67,2]	[0.6,0.34]	[2.66,1.87]	[0.59,0.36]
1.75	[2.3,1.8]	[0.48,0.41]	[2.3,1.61]	[0.48,0.49]
2	[2.08,1.57]	[0.31,0.49]	[2.08,1.3]	[0.31,0.46]
2.5	[1.89,1.1]	[0.32,0.3]	[1.88,1.02]	[0.33,0.13]
3	[1.53,1]	[0.5,0.06]	[1.54,1]	[0.5,0.01]

5. Comparative Studies

In traditional control under CS, it is known that a control chart having the smaller values of average run length (ARL) and standard deviation of run length (SDRL) is said to be efficient in detecting the shift in the process. In the neutrosophic theory, according to [29,30], a method is said to be efficient if it provides the parameter in the indeterminacy interval rather than the determined values in uncertainty. As mentioned by [32], a chart under the NS is said to be more efficient if it has smaller values of NARL than the competitor's charts. We will compare the efficiency of the proposed chart in NARL with the traditional Shewhart X-bar, EWMA X-bar chart proposed by [19] and chart proposed by [34] under NS. We will compare the performance of all the charts at the same specified neutrosophic parameters. Table 5 shows the NARL values of the control charts when $n_N \epsilon [3, 5]$, $ARL_{0N} \epsilon \{370, 370\}$, and $\lambda_N \epsilon [0.08, 0.12]$. We note that the proposed chart under the NS has smaller values of NARL as compared to the traditional Shewhart X-bar, EWMA X-bar chart [19] and charts proposed by [34]. For example, when $d = 0.05$, the NARL and NSD from the present chart are $ARL_{1N} \epsilon \{270.32, 248.92\}$ and $NSD \epsilon$ [257.15,238.27]; from [34], it is $ARL_{1N} \epsilon [356.86, 348.52]$, and from [19], they are charts 278 and 261, respectively. From this comparison, it is clear that the proposed chart has smaller values of NARL and NSD, which has the ability to detect a small shift in the process. The theoretical comparisons in NARL of the three charts show the superiority of the proposed control chart.

Table 5. The comparison between three charts.

	[19] Chart		Shewhart X-Bar Chart Under CS		Proposed Chart		[34]
	n= 3; λ	k = 2.715	n= 3; λ = 1.0	k = 3.01	$k_N\epsilon$ [2.655,2.765]; n= [3,5]; $\lambda_N\epsilon$[0.08,0.12]		$k_N\epsilon$ [3,3.001]; $\lambda_N\epsilon$[0.08,0.12].
d	ARL	SDRL	ARL	SDRL	NARL	NSD	NARL
0	371.865	348.837136	370.8831	354.4075	[368.28,376.77]	[345.26,354.91]	[370.08,370.11]
0.05	278.1253	261.774943	358.9364	340.3296	[270.32,248.92]	[257.15,238.27]	[356.86,348.52]
0.1	150.7524	140.816481	328.7539	317.8932	[141.33,117.16]	[130.78,106.3]	[321.83,295.53]
0.15	86.3401	77.451166	283.8335	280.105	[80.28,61.22]	[68.96,53.3]	[275.44,233.48]
0.2	53.6373	44.328357	234.1001	229.8941	[50.59,36.58]	[39.41,28.44]	[227.54,177.61]
0.25	36.4577	28.061015	194.5368	194.1908	[34.7,24.71]	[24.42,17.5]	[184.1,133.07]
0.3	26.9744	18.701549	150.8646	152.3704	[25.78,18.28]	[16.59,11.86]	[147.43,99.48]
0.4	16.8197	9.92102	97.1724	95.70603	[16.62,11.53]	[9.06,6.2]	[93.98,56.56]
0.5	12.0976	6.090614	62.5904	60.1786	[12.24,8.19]	[5.83,3.66]	[60.65,33.38]
0.6	9.2986	4.102965	41.1474	40.18904	[9.57,6.52]	[4,2.59]	[40.01,20.55]
0.7	7.6389	3.122736	27.6095	26.86251	[7.91,5.35]	[3.01,1.91]	[27.06,13.21]
0.8	6.4074	2.341447	19.2001	18.76261	[6.74,4.59]	[2.34,1.51]	[18.78,8.85]
0.9	5.5639	1.885225	13.5113	12.74982	[5.87,4]	[1.88,1.21]	[13.37,6.18]
1	4.9515	1.570858	9.811	9.239676	[5.17,3.58]	[1.55,1.02]	[9.76,4.49]

For the summated data, we suppose that $n_N \epsilon [3,5]$, $ARL_{0N} \epsilon \{370, 370\}$, and $\lambda_N \epsilon [0.08, 0.12]$. The 40 observations from NND are generated, having half of the data generated assuming that the process is in-control state, and next 20 observations are generated assuming that the process has shifted with $d = 0.25$. The simulated data along with $\overline{X}_N \epsilon \left\{ \overline{X}_L, \overline{X}_U \right\}$ and $EWMA_{N,i}$ are shown in Table 6. From Table 1, the tabulated NARL is $ARL_{1N} \epsilon \{24.42, 17.5\}$, so it is expected that the shift should be detected between the 17th sample and the 24th sample. We constructed Figure 1 for the proposed control chart, Figure 2 for the chart proposed by [34], and Figure 3 for the traditional Shewhart X-bar chart. From Figures 1–3, it is worth noting that the proposed control chart detects the shift in the process between the 17th sample and the 24th sample. Figure 2 shows that although the process is an in-control state, some points are in an indeterminacy interval. Figure 3 shows that the process is an in-control state, and all the parameters are determined. By comparing Figures 1–3, it is concluded that the proposed control under NS is quite effective, flexible, and efficient in detecting the shift in the process as compared to the existing control charts.

Table 6. The simulated neutrosophic data.

Sr#	$\overline{X}_N$	$EWMA_N$	Sr#	$\overline{X}_N$	$EWMA_N$
1	[73.99838,73.99999]	[73.99995,74.00009]	21	[73.99971,74.00165]	[73.99984,74.00022]
2	[73.99981,73.9995]	[73.99994,74.00002]	22	[73.99993,73.99948]	[73.99985,74.00013]
3	[74.00099,74.00014]	[74.00003,74.00004]	23	[74.00076,74.00065]	[73.99992,74.00019]
4	[74.00015,73.99811]	[74.00004,73.99981]	24	[73.9993,73.99972]	[73.99987,74.00014]
5	[74.00114,73.99979]	[74.00012,73.9998]	25	[73.99958,73.99998]	[73.99985,74.00012]
6	[74.00067,73.99963]	[74.00017,73.99978]	26	[74.00036,74.00098]	[73.99989,74.00022]
7	[74.00055,74.00081]	[74.0002,73.99991]	27	[74.0003,73.99988]	[73.99992,74.00018]
8	[74.00034,73.99897]	[74.00021,73.99979]	28	[74.00039,73.99945]	[73.99996,74.00009]
9	[73.99929,73.99955]	[74.00014,73.99976]	29	[74.00027,74.00025]	[73.99998,74.00011]
10	[73.99944,73.99988]	[74.00008,73.99978]	30	[73.99993,74.00118]	[73.99998,74.00024]
11	[74.00008,74.00013]	[74.00008,73.99982]	31	[74.00062,74.00047]	[74.00003,74.00027]
12	[73.99965,74.00038]	[74.00005,73.99989]	32	[74.00077,74.00038]	[74.00009,74.00028]
13	[74.00073,73.99959]	[74.0001,73.99985]	33	[73.99993,74.00014]	[74.00008,74.00026]
14	[73.99947,73.99942]	[74.00005,73.9998]	34	[74.00065,74.00044]	[74.00012,74.00029]
15	[73.99962,73.99951]	[74.00002,73.99977]	35	[73.99977,74.00121]	[74.00009,74.0004]
16	[73.99927,74.00025]	[73.99996,73.99982]	36	[74.00068,74.00122]	[74.00014,74.00049]
17	[74.00016,74.00104]	[73.99997,73.99997]	37	[74.00078,74.00129]	[74.00019,74.00059]
18	[74.00039,74.00034]	[74.00001,74.00001]	38	[74.00079,73.99968]	[74.00024,74.00048]
19	[73.99919,74.00029]	[73.99994,74.00005]	39	[73.99973,73.99953]	[74.0002,74.00037]
20	[73.99881,73.99987]	[73.99985,74.00003]	40	[74.00126,73.99959]	[74.00028,74.00027]

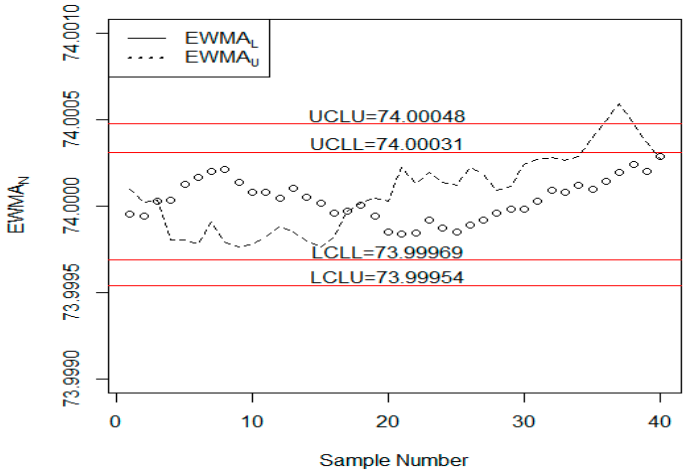

Figure 1. The proposed chart for the summated data.

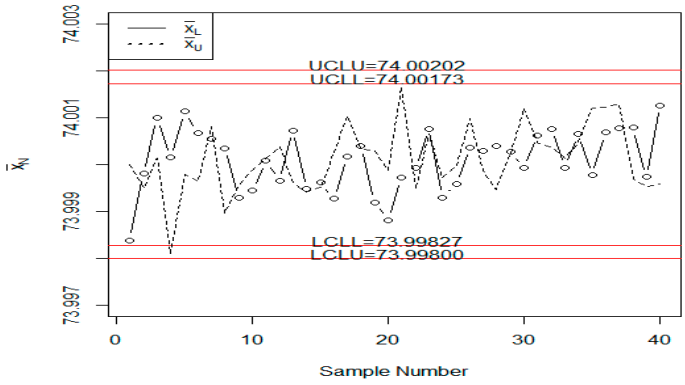

Figure 2. The Aslam and Khan (2019) chart for the summated data.

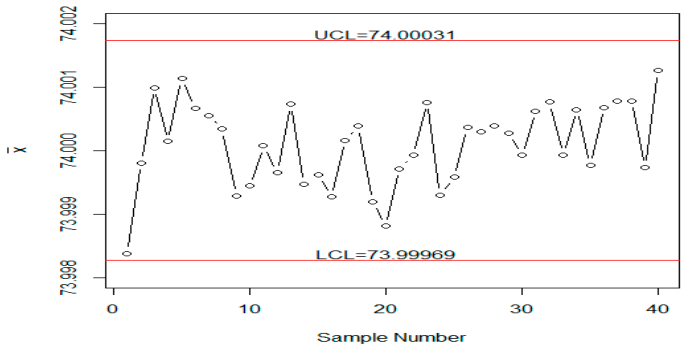

Figure 3. The X-bar chart under classic statistics (CS) for the summated data.

6. Application

A famous automobile industry situated in Saudi Arabia is interested in applying the proposed control chart under the NS for monitoring the production of engine piston rings (EPR). The EPR is an important part of the engine, which improves its efficiency by minimizing the gas or oil leakage and transforming the heat to the cylinder wall. The EPR is a continuous variable and has the possibility of imprecise, fuzzy, and in-determined values. In such a case, the use of the proposed control to monitor the production process of EPR using the proposed control chart under the NS will be more effective and informative than the use of the existing control chart. The proposed control chart will enhance the power of the monitoring of the process using the current sample and previous sample information. Furthermore, the simulation study showed the efficiency of the proposed chart over the existing chart proposed by Aslam and Khan [34]. Therefore, the use of the proposed control chart for the monitoring of ERP production in the industry will help in minimizing the non-conforming ERP product. Suppose that the automobile industry is interested in seeing the efficiency of the proposed chart when $n_N \epsilon [3, 5]$, $ARL_{0N} \epsilon \{370, 370\}$, and $\lambda_N \epsilon [0.12, 0.12]$. The neutrosophic control limit coefficient is $k_N \epsilon \{3.001, 3.002\}$. The neutrosophic data of ERP is taken from Aslam and Khan [34] and shown in Table 7 for easy reference. The neutrosophic statistic and neutrosophic control limits for monitoring the ERP data shown in Table 7 are $LCL_N \epsilon \{73.9964, 73.9969\}$; $\sigma_N \epsilon \{0.008896, 0.009399\}$ and $UCL_N \epsilon \{74.0051, 74.0055\}$; $\sigma_N \epsilon \{0.008896, 0.009399\}$. We constructed Figure 4 for the proposed control chart, Figure 5 for the chart proposed by Aslam and Khan [34], and Figure 6 for the traditional Shewhart X-bar chart. From Figures 4–6, it is noted that the proposed control chart shows that the process is near the neutrosophic target lines. On the other hand, the existing control chart by Aslam and Khan [34] shows much variation in the process. The traditional Shewhart has the determined values of parameters, and is not suitable in uncertainty. By comparing the three charts, it is concluded that the proposed chart has the ability to centralize EPR production process.

Table 7. The neutrosophic EPR data.

Sr#	Sample					$\bar{X}_N$	$EWMA_N$
1	[74.03,74.03]	[74.002,73.991]	[74.019,74.019]	[73.992,73.992]	[74.008,74.001]	[74.0102,74.0066]	[74.0023,74.0021]
2	[73.995,73.995]	[73.992,74.003]	[74.001,74.001]	[74.011,74.011]	[74.004,74.004]	[74.0006,74.0028]	[74.0021,74.0021]
3	[73.988,74.017]	[74.024,74.024]	[74.021,74.021]	[74.005,74.005]	[74.002,73.995]	[74.008,74.0124]	[74.0028,74.0028]
4	[74.002,74.002]	[73.996,73.996]	[73.993,73.993]	[74.015,74.015]	[74.009,74.009]	[74.003,74.003]	[74.0028,74.0028]
5	[73.992,73.992]	[74.007,74.007]	[74.015,74.015]	[73.989,73.989]	[74.014,73.998]	[74.0034,74.0002]	[74.0029,74.0013]
6	[74.009,74.009]	[73.994,74.001]	[73.997,73.997]	[73.985,73.985]	[73.993,73.993]	[73.9956,73.997]	[74.002,74.0008]
7	[73.995,73.998]	[74.006,74.006]	[73.994,73.994]	[74,74]	[74.005,74.005]	[74,74.0006]	[74.0018,74.0013]
8	[73.985,73.985]	[74.003,74.01]	[73.993,73.993]	[74.015,74.015]	[73.988,73.988]	[73.9968,73.9982]	[74.0012,74.001]
9	[74.008,74.005]	[73.995,73.995]	[74.009,74.009]	[74.005,74.005]	[74.004,74.004]	[74.0042,74.0036]	[74.0015,74.0017]
10	[73.998,73.998]	[74,74]	[73.99,73.99]	[74.007,74.007]	[73.995,73.995]	[73.998,73.998]	[74.0011,74.0013]
11	[73.994,73.998]	[73.998,73.998]	[73.994,73.994]	[73.995,73.995]	[73.99,74.001]	[73.9942,73.9972]	[74.0003,74.0009]
12	[74.004,74.004]	[74,74.002]	[74.007,74.005]	[74,74.001]	[73.996,73.996]	[74.0014,74.0016]	[74.0004,74.001]
13	[73.983,73.993]	[74.002,74.002]	[73.998,73.998]	[73.997,73.997]	[74.012,74.005]	[73.9984,73.999]	[74.0002,74.0011]
14	[74.006,74.006]	[73.967,73.985]	[73.994,73.994]	[74,74]	[73.984,73.996]	[73.9902,73.9962]	[73.999,74.0006]
15	[74.012,74.012]	[74.014,74.012]	[73.998,73.998]	[73.999,73.999]	[74.007,74.007]	[74.006,74.0056]	[73.9998,74.0019]
16	[74,74]	[73.984,73.984]	[74.005,74.005]	[73.998,73.998]	[73.996,73.996]	[73.9966,73.9966]	[73.9994,74.0013]
17	[73.994,73.994]	[74.012,74.012]	[73.986,73.986]	[74.005,74.005]	[74.007,74.007]	[74.0008,74.0008]	[73.9996,74.0014]
18	[74.006,74.006]	[74.01,74.011]	[74.018,74.018]	[74.003,74.003]	[74,74.001]	[74.0074,74.0078]	[74.0005,74.0021]
19	[73.984,73.984]	[74.002,74.002]	[74.003,74.003]	[74.005,74.005]	[73.997,73.997]	[73.9982,73.9982]	[74.0003,74.0011]
20	[74]	[74.01,74.01]	[74.013,74.009]	[74.02,74.015]	[74.003,74.003]	[74.0092,74.0074]	[74.0013,74.0018]
21	[73.982,73.982]	[74.001,74.001]	[74.015,74.015]	[74.005,74.005]	[73.996,73.996]	[73.9998,73.9998]	[74.0011,74.0012]
22	[74.004,74.004]	[73.999,73.999]	[73.99,73.99]	[74.006,74.006]	[74.009,74.002]	[74.0016,74.0002]	[74.0012,74.0011]
23	[74.01,74.01]	[73.989,73.989]	[73.99,73.99]	[74.009,74.005]	[74.014,74.011]	[74.0024,74.001]	[74.0013,74.0014]
24	[74.015,74.011]	[74.008,74.008]	[73.993,73.993]	[74,74]	[74.01,74.011]	[74.0052,74.0046]	[74.0018,74.0018]
25	[73.982,73.982]	[73.984,73.989]	[73.995,73.995]	[74.017,74.012]	[74.013,74.01]	[73.9982,73.9976]	[74.0014,74.001]

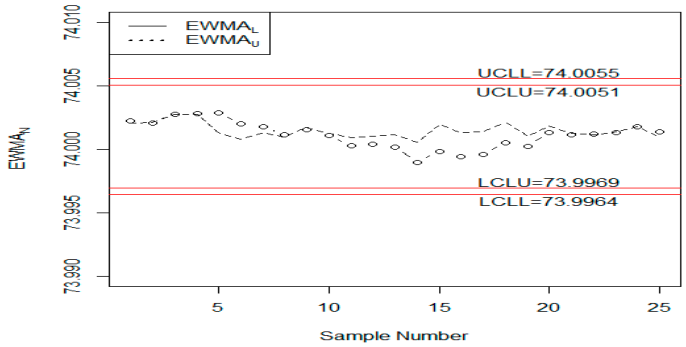

Figure 4. The proposed chart for the real data.

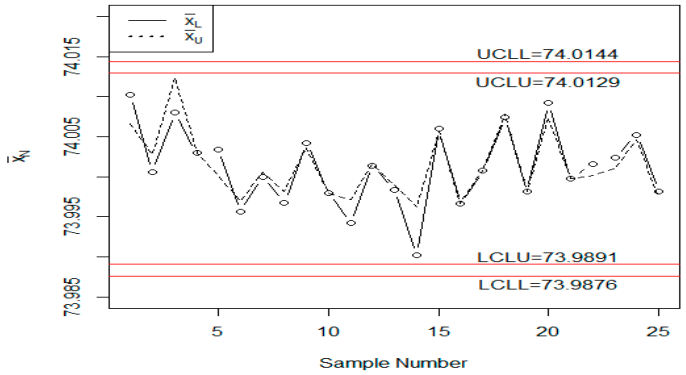

Figure 5. The Aslam and Khan (2019) chart for the real data.

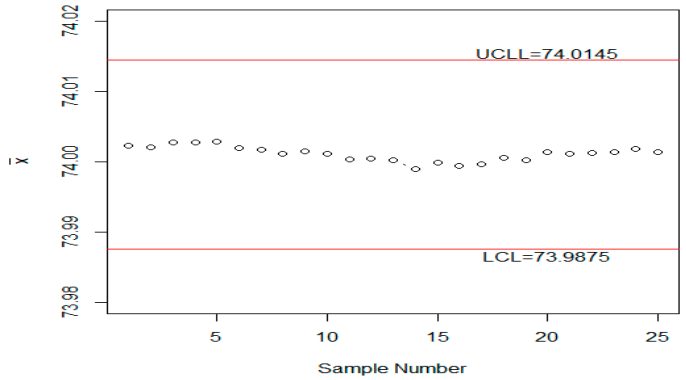

Figure 6. The X-bar chart under CS for the real data.

7. Concluding Remarks

We presented the designing of the X-bar control chart using the neutrosophic EWMA (NEWMA) statistics. The neutrosophic NEWMA and NMSC are introduced in this paper. Some tables for various neutrosophics are presented for practical use in the industry. The theoretical comparisons in the NARL and simulation study showed that the proposed chart performs better than the competitor's charts. The real example of ERP data from the automobile industry also showed the efficiency of the proposed chart. We recommend using the proposed control chart for monitoring the process in the automobile, aerospace, mobiles, water drinking, and medical instrument industries. The proposed chart can be only applied when the variable of interest follows the neutrosophic normal distribution. The proposed chart using some non-normal distributions can be considered as future research. The proposed control chart using some advanced sampling schemes will be considered as future research.

Author Contributions: M.A.; A.H.A.-M. and N.K. conceived and designed the experiments; M.A. and N.K. performed the experiments; M.A. and N.K. analyzed the data; M.A. contributed reagents/materials/analysis tools; M.A. wrote the paper.

Funding: This work was funded by the Deanship of Scientific Research (DSR), King Abdulaziz University, Jeddah. The author, therefore, gratefully acknowledges the DSR technical and financial support.

Acknowledgments: The authors are deeply thankful to the editor and reviewers for their valuable suggestions to improve the quality of this manuscript.

Conflicts of Interest: The authors declare no conflict of interest regarding this paper.

References

1. Senturk, S.; Erginel, N. Development of fuzzy $\bar{X}$~-R~ and $\bar{X}$~-S~ control charts using α-cuts. *Inf. Sci.* **2009**, *179*, 1542–1551. [CrossRef]
2. Hart, M.K.; Lee, K.Y.; Hart, R.F.; Robertson, J.W. Application of Attribute Control Charts to Risk-Adjusted Data for Monitoring and Improving Health Care Performance. *Qual. Manag. Healthc.* **2003**, *12*, 5–19. [CrossRef]
3. Bai, D.; Lee, K. Variable sampling interval X control charts with an improved switching rule. *Int. J. Prod. Econ.* **2002**, *76*, 189–199. [CrossRef]
4. Castagliola, P.; Celano, G.; Fichera, S.; Nunnari, V. A variable sample size S2-EWMA control chart for monitoring the process variance. *Int. J. Reliab. Qual. Saf. Eng.* **2008**, *15*, 181–201. [CrossRef]
5. Panthong, C.; Pongpullponsak, A. Non-Normality and the Fuzzy Theory for Variable Parameters Control Charts. *Thai J. Math.* **2016**, *14*, 203–213.
6. Pereira, P.; Seghatchian, J.; Caldeira, B.; Xavier, S.; de Sousa, G. Statistical methods to the control of the production of blood components: Principles and control charts for variables. *Transfus. Apher. Sci.* **2018**, *57*, 132–142. [CrossRef]
7. Roberts, S. Control chart tests based on geometric moving averages. *Technometrics* **1959**, *1*, 239–250. [CrossRef]
8. Haq, A. An improved mean deviation exponentially weighted moving average control chart to monitor process dispersion under ranked set sampling. *J. Stat. Comput. Simul.* **2014**, *84*, 2011–2024. [CrossRef]
9. Haq, A.; Brown, J.; Moltchanova, E. New exponentially weighted moving average control charts for monitoring process mean and process dispersion. *Qual. Reliab. Eng. Int.* **2015**, *31*, 877–901. [CrossRef]
10. Haq, A.; Brown, J.; Moltchanova, E.; Al-Omari, A.I. Effect of measurement error on exponentially weighted moving average control charts under ranked set sampling schemes. *J. Stat. Comput. Simul.* **2015**, *85*, 1224–1246. [CrossRef]
11. Abbasi, S.A.; Riaz, M.; Miller, A.; Ahmad, S.; Nazir, H.Z. EWMA dispersion control charts for normal and non-normal processes. *Qual. Reliab. Eng. Int.* **2015**, *31*, 1691–1704. [CrossRef]
12. Abbasi, S.A. Exponentially weighted moving average chart and two-component measurement error. *Qual. Reliab. Eng. Int.* **2016**, *32*, 499–504. [CrossRef]
13. Sanusi, R.A.; Riaz, M.; Adegoke, N.A.; Xie, M. An EWMA monitoring scheme with a single auxiliary variable for industrial processes. *Comput. Ind. Eng.* **2017**, *114*, 1–10. [CrossRef]
14. Montgomery, D.C. *Introduction to Statistical Quality Control*; John Wiley & Sons: Hoboken, NJ, USA, 2007.
15. Arshad, W.; Abbas, N.; Riaz, M.; Hussain, Z. Simultaneous use of runs rules and auxiliary information with exponentially weighted moving average control charts. *Qual. Reliab. Eng. Int.* **2017**, *33*, 323–336. [CrossRef]
16. Adeoti, O.A. A new double exponentially weighted moving average control chart using repetitive sampling. *Int. J. Qual. Reliab. Manag.* **2018**, *35*, 387–404. [CrossRef]
17. Adeoti, O.A.; Malela-Majika, J.-C. Double exponentially weighted moving average control chart with supplementary runs-rules. *Qual. Technol. Quant. Manag.* **2019**, 1–24. [CrossRef]
18. Hunter, J.S. The exponentially weighted moving average. *J. Qual. Technol.* **1986**, *18*, 203–210. [CrossRef]
19. Lucas, J.M.; Saccucci, M.S. Exponentially weighted moving average control schemes: Properties and enhancements. *Technometrics* **1990**, *32*, 1–12. [CrossRef]
20. Khademi, M.; Amirzadeh, V. Fuzzy rules for fuzzy $\overline{X}$ and R control charts. *Iran. J. Fuzzy Syst.* **2014**, *11*, 55–66.
21. Faraz, A.; Moghadam, M.B. Fuzzy control chart a better alternative for Shewhart average chart. *Qual. Quant.* **2007**, *41*, 375–385. [CrossRef]
22. Zarandi, M.F.; Alaeddini, A.; Turksen, I. A hybrid fuzzy adaptive sampling–run rules for Shewhart control charts. *Inf. Sci.* **2008**, *178*, 1152–1170. [CrossRef]

23. Faraz, A.; Kazemzadeh, R.B.; Moghadam, M.B.; Bazdar, A. Constructing a fuzzy Shewhart control chart for variables when uncertainty and randomness are combined. *Qual. Quant.* **2010**, *44*, 905–914. [CrossRef]
24. Wang, D.; Hryniewicz, O. A fuzzy nonparametric Shewhart chart based on the bootstrap approach. *Int. J. Appl. Math. Comput. Sci.* **2015**, *25*, 389–401. [CrossRef]
25. Kahraman, C.; Gülbay, M.; Boltürk, E. *Fuzzy Shewhart Control Charts, Fuzzy Statistical Decision-Making*; Springer: Berlin/Heidelberg, Germany, 2016; pp. 263–280.
26. Khan, M.Z.; Khan, M.F.; Aslam, M.; Niaki, S.T.A.; Mughal, A.R. A Fuzzy EWMA Attribute Control Chart to Monitor Process Mean. *Information* **2018**, *9*, 312. [CrossRef]
27. Smarandache, F. Neutrosophic Logic-A Generalization of the Intuitionistic Fuzzy Logic. *Multispace Multistructure Neutrosophic Transdiscipl.* **2010**, *4*, 396. [CrossRef]
28. Smarandache, F. *Introduction to Neutrosophic Statistics*; Sitech & Education: Columbus, OH, USA, 2014.
29. Chen, J.; Ye, J.; Du, S. Scale effect and anisotropy analyzed for neutrosophic numbers of rock joint roughness coefficient based on neutrosophic statistics. *Symmetry* **2017**, *9*, 208. [CrossRef]
30. Chen, J.; Ye, J.; Du, S.; Yong, R. Expressions of rock joint roughness coefficient using neutrosophic interval statistical numbers. *Symmetry* **2017**, *9*, 123. [CrossRef]
31. Aslam, M. A New Sampling Plan Using Neutrosophic Process Loss Consideration. *Symmetry* **2018**, *10*, 132. [CrossRef]
32. Aslam, M.; Bantan, R.A.; Khan, N. Design of a new attribute control chart under neutrosophic statistics. *Int. J. Fuzzy Syst.* **2019**, *21*, 433–440. [CrossRef]
33. Aslam, M.; Khan, N.; Khan, M. Monitoring the Variability in the Process Using Neutrosophic Statistical Interval Method. *Symmetry* **2018**, *10*, 562. [CrossRef]
34. Aslam, M.; Khan, N. A new variable control chart using neutrosophic interval method-an application to automobile industry. *J. Intell. Fuzzy Syst.* **2019**, *36*, 2615–2623. [CrossRef]
35. Aslam, M.; Khan, N.; Albassam, M. Control Chart for Failure-Censored Reliability Tests under Uncertainty Environment. *Symmetry* **2018**, *10*, 690. [CrossRef]
36. Aslam, M. Attribute Control Chart Using the Repetitive Sampling under Neutrosophic System. *IEEE Access* **2019**, *7*, 15367–15374. [CrossRef]
37. Aslam, M. Control Chart for Variance using Repetitive Sampling under Neutrosophic Statistical Interval System. *IEEE Access* **2019**, *7*, 25253–25262. [CrossRef]
38. Şentürk, S.; Erginel, N.; Kaya, İ.; Kahraman, C. Fuzzy exponentially weighted moving average control chart for univariate data with a real case application. *Appl. Soft Comput.* **2014**, *22*, 1–10. [CrossRef]